mew and G. Paik, *J. Bacteriol.* **92**, 635 (1966). See also the data on the survival of five different bacteria under deep-sea conditions summarized in table 2 (p. 289) of (*17*).
16. R. E. Marquis, *Adv. Microb. Physiol.* **14**, 159 (1976).
17. R. Y. Morita, in *Survival of Vegetative Microbes*, T. R. G. Gray and J. R. Postgate, Eds. (Cambridge Univ. Press, Cambridge, England, 1976), pp. 279–298.
18. M. R. Heinrich, Ed., *Extreme Environments: Mechanisms of Microbial Adaptation* (Academic Press, New York, 1976).
19. R. Singleton, Jr., C. R. Middaugh, R. D. MacElroy, *Int. J. Pept. Protein Res.* **10**, 39 (1977); R. Singleton, Jr., and R. E. Amelunxen, *Bacteriol. Rev.* **37**, 320 (1973).
20. We are indebted to Prof. C. E. ZoBell for his loan of pressure vessels and for his comments on the manuscript. Supported by contract No. 07-7911 from Sandia Laboratories (a prime contractor of the U.S. Department of Energy) and by grant OCE 76-12017 from the National Science Foundation.

8 December 1978; revised 9 April 1979

Voltage-Dependent Calcium and Potassium Ion Conductances: A Contingency Mechanism for an Associative Learning Model

Abstract. *Persistent light-induced depolarization results from Ca^{2+} influx across a photoreceptor membrane. The marked dependence on potential of this Ca^{2+} influx and a Ca^{2+}-dependent K^+ efflux accounts for enhancement of the light-induced depolarization when light is paired with rotation. A positive feedback cycle between light-induced depolarization and synaptic depolarization due to stimulus pairing can explain long-lasting behavioral changes produced by associative training but not control paradigms. The sensitivity of this Ca^{2+} influx to intracellular levels of adenosine 3′,5′-monophosphate suggests biochemical steps for this model of associative learning.*

Learning, as it has been most generally defined, refers to a change of an animal's behavior as a result of training. Specific definitions of learning have been quite different, depending on the viewpoints and interests of individual investigators. Habituation, the decrement of a behavioral response with repetition, has been regarded by some as a simple form of learning. Others require in their definitions features of associative learning (*1*) such as pairing specificity or contingency, acquisition, retention, and stimulus specificity.

It cannot be assumed that these phenomena (habituation, sensitization, conditioning, and so forth) depend on common neurophysiologic and biochemical mechanisms. It is quite reasonable that the training regimens and neural networks important for a nonassociative process such as habituation involve cellular bases different from those that underlie associative learning.

One approach to the study of cellular mechanisms responsible for learning is to use relatively unevolved species that have fairly uncomplicated neural systems. Changes within these neural systems are sought as they relate to behavioral changes produced by training procedures.

An outstanding disadvantage of these species for this approach has been their rather limited capacity for learned behavior. Yet, for any possible generalizability of mechanisms uncovered in "simple" neural systems, the learned behavior should closely resemble that of higher organisms. Learning behavior of gastropod molluscs (which have "simple" neural systems) cannot be identically compared to the sophisticated learning (such as conditioning) of which primates are capable. However, enough might be found in common for learned behavior of lower organisms and more evolved species to direct our attention to common biologic principles.

In previous studies, I have found that movement of the Pacific nudibranch *Hermissenda crassicornis* toward a light source is markedly reduced after repeated pairing of a light stimulus with rotation (*2*). Crow and Alkon showed that this behavioral change is associative (that is, randomized light and rotation do not produce the same effect), persists for at least several days after training, and increases with practice (*2*). Specificity of this training effect was suggested by the fact that trained animals did not show changes in responsiveness to food (*3*). Thus, this behavioral change of *Hermissenda* shares defining features of, and can serve as a model for, associative learning (*3*).

Because of the relative simplicity of the *Hermissenda* nervous system it has been possible to ascertain many of the invariant aspects of the three sensory pathways essential to the associative learning model: the visual, statocyst, and chemosensory pathways (*4*). These three sensory pathways interact with each other, but are selectively responsive to the sensory stimuli (light, rotation, and food) used for the training and control procedures (*4, 5*). Within these neural systems of *Hermissenda* specific changes occurred only in animals subjected to associative training paradigms and not to control paradigms (*5, 6*).

A possibly primary neural change (which could account for the other changes within the networks) occurred within the type B photoreceptor (*6*). This involved, in part, persistent depolarization and increased membrane resistance of this cell. I describe here how this cell, through its receptor and membrane properties, in addition to its synaptic relationships, provides for the associative nature or contingency of the associative learning model. The sensitivity of this cellular mechanism for contingency to intracellular adenosine 3′,5′-monophosphate (cyclic AMP) also suggests biochemical mechanisms for the behavioral changes produced by the associative training procedure.

There are three type B (and two type A) photoreceptors in each of two *Hermissenda* eyes. These photoreceptors have identifiable loci, geometries, and electrophysiologic characteristics (*4*). The type B photoreceptor, located in the anterodorsal portion of the eye, is ~ 35 μm in diameter. Its axon, ~ 1 μm in diameter, leaves the base of the eye, enters the optic nerve, passes ensheathed through the optic ganglion (for ~ 50 μm), enters the optic tract, and terminates in a spray of fine endings ~ 20 μm from its point of entry into the cerebropleural ganglion. Simultaneous intraaxonal and intrasoma recordings (*4*) and lesion experiments indicate that the generator potential arises at the rhabdome of the cell body and spreads passively down the axon. Impulses arise within the axon near the cerebropleural ganglion point of entry but do not actively invade the cell body. Synaptic interactions only occur at the terminal endings.

Thus, a lesion (cut nerve) proximal to the impulse-generating zone leaves a cell body that contains the phototransduction apparatus without impulses or synaptic interactions. Voltage and current clamp recordings can then be made with two electrodes in the cell body under favorable space-clamp conditions (*7*).

Type B photoreceptors in cut nerve preparations depolarize for 1 to 2 minutes (Fig. 1A) after a 30-second light step of moderate intensity (10^3 to 10^4 erg cm^{-2} sec^{-1}). This long-lasting depolarization (LLD) was always associated with a membrane resistance 1.5 to 3 times higher than the resting or dark value (*8*). Positive current injection, causing depolarization comparable to that produced by light, was not followed by an LLD or increased membrane resistance. With sufficient hyperpolarization during the light

0036-8075/79/0824-0810$00.50/0

response, however, the LLD and its associated conductance decrease could be eliminated. These observations suggested that the LLD arises from a voltage-dependent decrease of K^+ conductance (*8*). This LLD increased when the light step was paired with rotation (*8*); this increase with pairing could be due to the LLD's voltage dependence. These light and rotation stimuli were essentially identical to the stimuli that, when presented repeatedly to intact animals and isolated nervous systems, cause behavioral and neural changes (*5, 6*). To better understand the LLD and its increase with stimulus pairing, I recorded from type B cells under current and voltage-clamp conditions.

Techniques of intracellular recording and details of animal supply and maintenance were as described (*4, 5, 7*). Voltage clamp was effected with two microelectrodes, one for current injection, the other for voltage recording (*9*). Current was monitored simultaneously by a bath virtual ground amplifier and as the voltage drop on the current passing electrode. The settling time of the clamp apparatus was 3 to 5 msec. During light-induced photoreceptor responses under voltage clamp, no voltage changes (≥ 20 μV) were observed. Voltage-clamp measurements were made at different holding potentials after at least 15 seconds at each potential in the dark. No obvious differences in response to light were observed when a voltage-clamp series was made at sequentially more positive (or negative) holding potentials as compared to returning to the resting membrane potential (RP $\cong -55$ mV) after a light step at each test holding potential (*7, 10*). For many preparations it was possible to use two or three different external bathing solutions for the same cell. However, for each treatment condition a voltage-clamp analysis was made for at least five photoreceptors that had no previous treatment. The total number of photoreceptors studied was 65. All records presented here were made on a Brush pen recorder (*11*) (Gould, Inc., Cleveland, Ohio). Light stimuli (*12*) were provided by a tungsten 6-V, 15-W bulb (Philips, Netherlands). Light stimuli were repeated at 2-minute intervals after 10 minutes of dark adaptation.

Under voltage clamp of the type B photoreceptor in artificial seawater (ASW) (*13*), a large initial transient inward current and a much smaller sustained inward current appeared during a 30-second light step (Fig. 1B). The initial transient inward current reached its maximum value ~ 200 msec after light onset and rapidly decreased from its peak amplitude. This initial inward current was almost entirely eliminated (Fig. 1, D and E) by replacing external Na^+

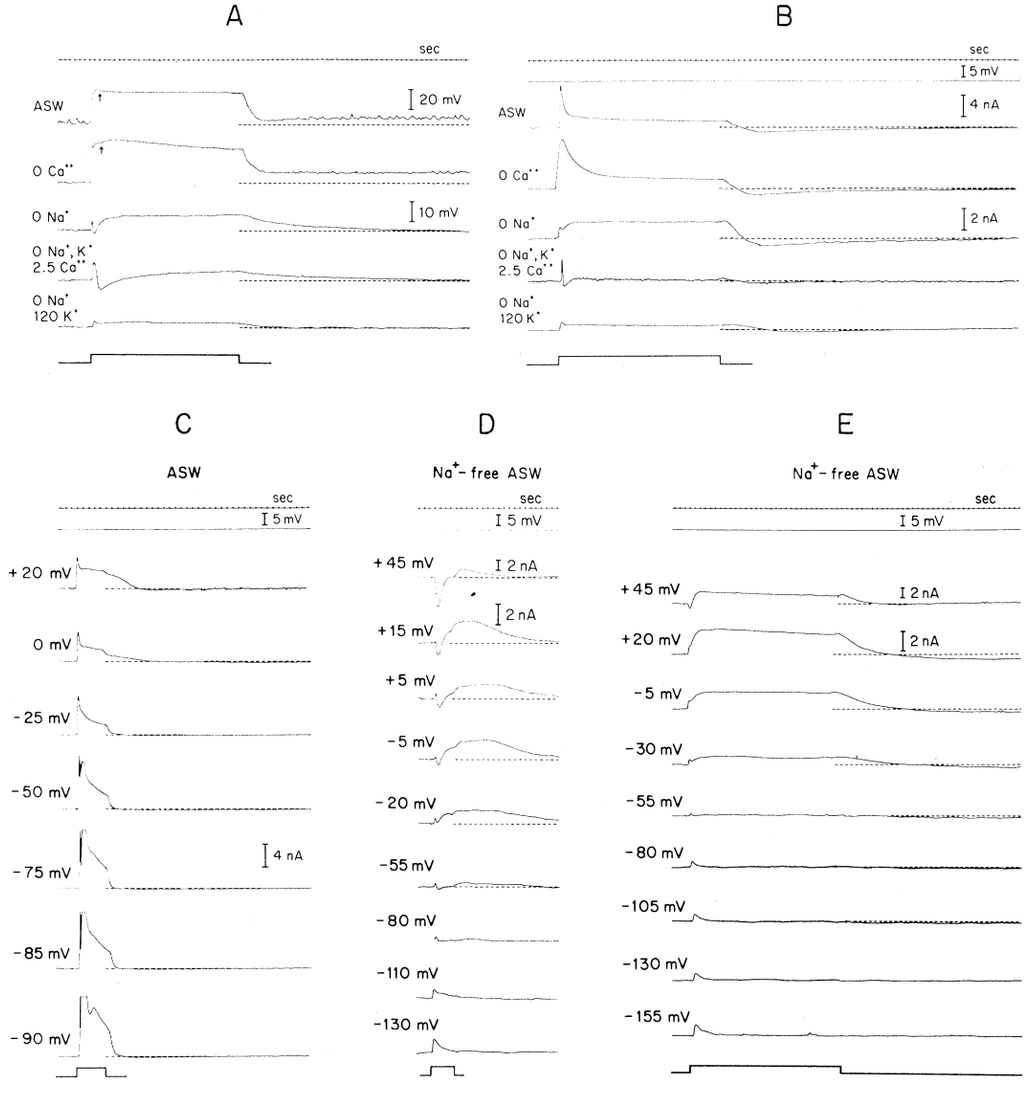

Fig. 1. Voltage and voltage-clamp recordings during and after light steps. (A) Voltage recordings of type B cells during and after a light step. Isolated nervous systems were bathed in artificial seawater (ASW); Ca^{2+}-free ASW; Na^+-free ASW; K^+-free ASW containing 2.5 m*M* Ca^{2+} and 65 m*M* Mg^{2+}; Na^+-free ASW containing 120 m*M* K^+. Dashed lines indicate level of resting membrane potential (RP). (B to E) Voltage-clamp recordings; up = inward current. Values at left are absolute holding potentials. Dashed lines indicate steady-state current in darkness for each holding potential. Voltage traces at top were recorded simultaneously with current (flowing from reference element in the bath) recordings. Lowest trace in each set indicates duration of light step. The upper two recordings in (A) and (B) were all from the same cell. All responses in (B) were recorded at the same holding potential: -20 mV. A sustained inward current (Ca^{2+}) is induced by light at holding potentials > RP in Na^+-free ASW. Most important, the sustained inward current (Ca^{2+}) is still present (B) in 120 m*M* K^+, Na^+-free ASW at -20 mV, which is the approximate reversal potential for the outward K^+ currents (Fig. 2C). The early outward current (K^+) is marked at higher light intensity (D). Light intensity: in (C) and (D), 1.8×10^6 erg cm^{-2} sec^{-1} (unfiltered); in (A), (B), and (E): 1.1×10^6 erg cm^{-2} sec^{-1} (unfiltered). Paper recording amplifier (*11*) saturates for some records of (C).

with equimolar tetramethylammonium (TMA), while the sustained inward current was largely unaffected. This sustained inward current, as it appeared in Na^+-free ASW, reached its peak amplitude in ~ 1 second and maintained its maximum amplitude throughout the light step. It appeared to increase slightly at the cessation of the step and decreased slowly for 5 to 7 seconds thereafter (Fig. 1, B, D, and E).

The initial transient inward current increased at holding potentials more negative than the RP and decreased at holding potentials more positive than RP (Fig. 1C). The sustained inward current, however, did not occur at holding potentials less than RP (Fig. 1, D and E), increased at more positive holding potentials up to +80 mV, and decreased with still more positive holding potentials (Fig. 2, B and D).

These observations can be explained by an increase during light of an inward Na^+ current (initial transient) and an inward voltage-dependent Ca^{2+} current (sustained). Additional experiments gave further confirmation of this explanation. The reversal potential of the putative Na^+ current, as extrapolated from the linear portion of its current-voltage relation (Figs. 1C and 2A) was ~ +60 mV. The nonlinearity of the relation was probably due to contamination by the voltage-dependent putative Ca^{2+} current (Fig. 2, B and D).

An initial small inward current in Na^+-free ASW became more apparent (Fig. 1, D and E) at holding potentials progressively more negative than the RP of the cell. This small inward current had a time course similar to that of the putative Na^+ current in ASW and thus may represent a residual Na^+ current. This residual initial inward current in Na^+-free ASW also increased somewhat (Fig. 1B) when external Ca^{2+} was reduced (2.5 m*M*) and external Mg^{2+} elevated (65 m*M*). The initial inward current also increased somewhat and inactivated more slowly when external Ca^{2+} was replaced in ASW with equimolar TMA (Fig. 1B).

In Na^+-free ASW the putative Ca^{2+} current (*14*) was reduced by lowering external Ca^{2+} in the bathing medium and was largely eliminated when external Ca^{2+} was lowered to 2.5 m*M*, while external Mg^{2+} was raised to 65 m*M* and external K^+ lowered to zero (Fig. 1, A and B). The Ca^{2+} current was also reduced 25 to 40 percent in ASW containing 1 m*M* $NiCl_2$ (Fig. 4C), as has been reported for other Ca^{2+} currents (*15*). This putative Ca^{2+} current, however, was not affected by intracellular injection of tetraethylammonium (TEA) ions (see below for conditions). Finally, intracellular iontophoresis (under voltage clamp and with no voltage change) of cyclic AMP (−0.5 nA through the voltage-recording electrode for 1 minute) reduced the amplitude of the Ca^{2+} current (in Na^+-free ASW) by 30 to 50 percent while iontophoresis (under identical conditions) of 5′-AMP had little or no effect (Fig. 3A). The same results were obtained when injection was performed under current clamp conditions (Fig. 3, B and C). [Under current clamp conditions in Na^+-free ASW the voltage-dependence of the Ca^{2+}-mediated voltage responses to light was also apparent (Fig. 3C).] Cyclic AMP had no clear effect on either membrane resistance or potential in the dark.

During light a transient outward current was also clearly apparent in Na^+-free ASW only with more intense light stimuli (Fig. 3, A and B). With less intense 30-second light steps this outward current could be observed in Na^+-free ASW containing 2.5 m*M* Ca^{2+}, 65 m*M* Mg^{2+}, and no K^+ (Fig. 1B). Under these conditions the outward current reached its peak amplitude 1 to 2 seconds after light onset and decreased to approximately zero within 4 seconds after light onset. In Na^+-free ASW with normal Ca^{2+} and Mg^{2+}, a small outward current occurred as a notch which also reached its peak amplitude 1 to 2 seconds after light onset (Fig. 1E). With a brighter light step the reversal potential in Na^+-free ASW of the outward current was ~ −80 MV (Figs. 1D and 2B). This is comparable to the reversal potential measured out of voltage clamp for the hyperpolarizing wave within the light response of the photoreceptor (*16*). The reversal potential of the outward current became more positive (~ −20 mV) when external K^+

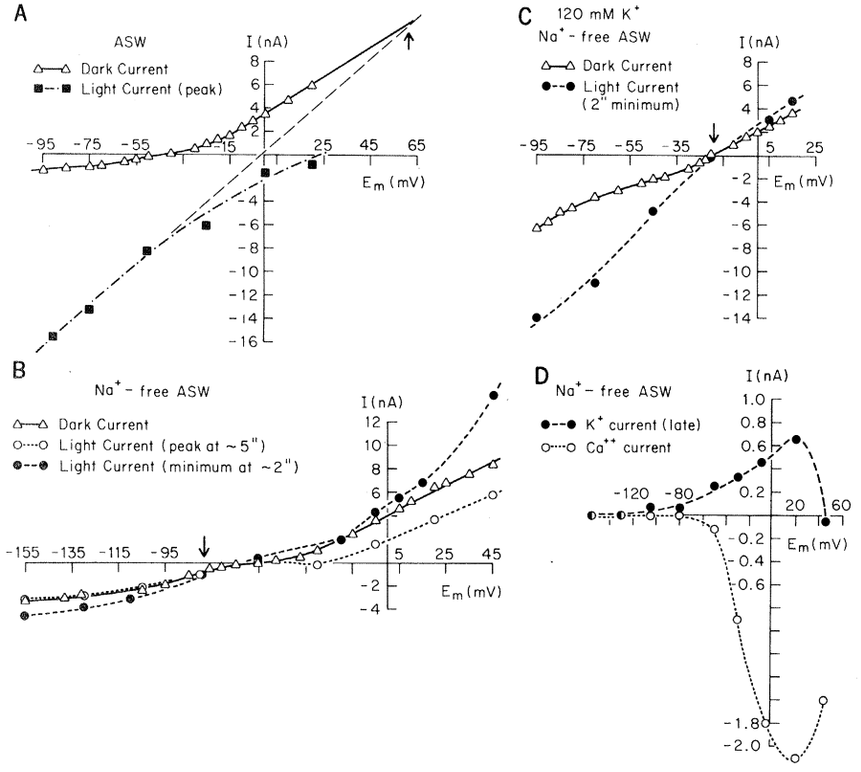

Fig. 2. Current-voltage plots from voltage-clamp recordings in darkness and during and after light steps (unfiltered); negative current = inward current. (A) Dark current and maximum initial inward current (Na^+) in ASW in response to 1.8×10^6 erg cm^{-2} sec^{-1} at different holding potentials. Arrow indicates reversal potential extrapolated from linear portion of current-voltage of I-V plot of Na^+ current. Plots are for recordings illustrated in Fig. 1C. (B) Dark current and isochronal (2 and 5 seconds after light onset) values of initial outward current (K^+) and sustained inward current (Ca^{2+}) in Na^+-free ASW in response to 1.8×10^6 and 1.1×10^6 erg cm^{-2} sec^{-1}, respectively, at different holding potentials. Plots are from recordings illustrated in Fig. 1D (outward current) and Fig. 1E (sustained inward current). There is no measurable sustained inward current at holding potentials < RP. (C) Dark current and isochronal (2 seconds after light onset) value of initial outward current (K^+) in 120 m*M* K^+ in Na^+-free ASW in response to 1.8×10^6 erg cm^{-2} sec^{-1} at different holding potentials. Reversal potential (arrow) of outward current has shifted toward more positive holding potential. (D) Absolute values of sustained light-induced inward current (Ca^{2+}) and late outward current (K^+) as a function of holding potential. Ca^{2+} value was measured 3 seconds after light step cessation; K^+ value, at 35 seconds after light step cessation. Note the parallel relation of the two currents to holding potential. Light intensity, 1.1×10^6 erg cm^{-2} sec^{-1}. Values are taken from recordings illustrated in Fig. 1E.

was raised (Fig. 2C) to 120 m*M* in Na^+-free ASW (adjusted with TMA to maintain equimolarity). The outward current was almost eliminated when 4 m*M* 4-aminopyridine was added to the bathing medium (Fig. 4C). This concentration of 4-aminopyridine also reduced the putative Na^+ current but had little effect on the sustained putative Ca^{2+} current (Fig. 4C). The outward current was also reduced by iontophoresis under voltage clamp of TEA (−1.0 nA through the voltage recording electrode for 2 minutes). Addition of Ni^{2+} (1 m*M*) also greatly reduced the outward current while reducing but not eliminating the putative Na^+ current (Fig. 4, A to C). These observations indicated that the light-induced outward current is carried by K^+ ions. The effect of Ni^{2+} on this putative K^+ current is consistent with previous reports (*17*) that a light-induced K^+ current (in *Hermissenda* photoreceptors) results from increased intracellular Ca^{2+}. Ca^{2+}-dependent K^+ currents have been reported in other preparations (*18*).

To summarize, the three currents induced during a light step were most likely carried by Na^+ (a rapidly decreasing inward current), K^+ (a rapidly decreasing outward current), and Ca^{2+} (a sustained inward current which decreased slowly following the cessation of the light step). After a light step, there was a prolonged outward current (Fig. 1B). This current increased with holding potentials more positive than RP and became small but did not entirely disappear with more negative holding potentials in ASW and in Na^+-free ASW (Fig. 1E). At holding potentials ≥ +45 mV in Na^+-free ASW the late outward current began to decrease (Fig. 2D). The late outward current was eliminated by 4 m*M* 4-aminopyridine (Fig. 4C), intracellular TEA injection (see above for conditions), and 1 m*M* Ni^{2+} added to ASW. These data indicate that the late outward current at holding potentials ≥ RP is a K^+ current which depends on a light-induced Ca^{2+} current. The Ca^{2+} current induced during light had a slow recovery after the light step. After the light step in 4-aminopyridine, when there was no apparent late outward current, there was a prolonged slowly recovering inward current, presumably Ca^{2+}, which was quite potential-dependent (Fig. 4C). Thus, following a light step, a substantial prolonged Ca^{2+} current (most apparent in 4-aminopyridine) will occur only at holding potentials > RP. The K^+ current (or currents), therefore, could be enhanced by intra-

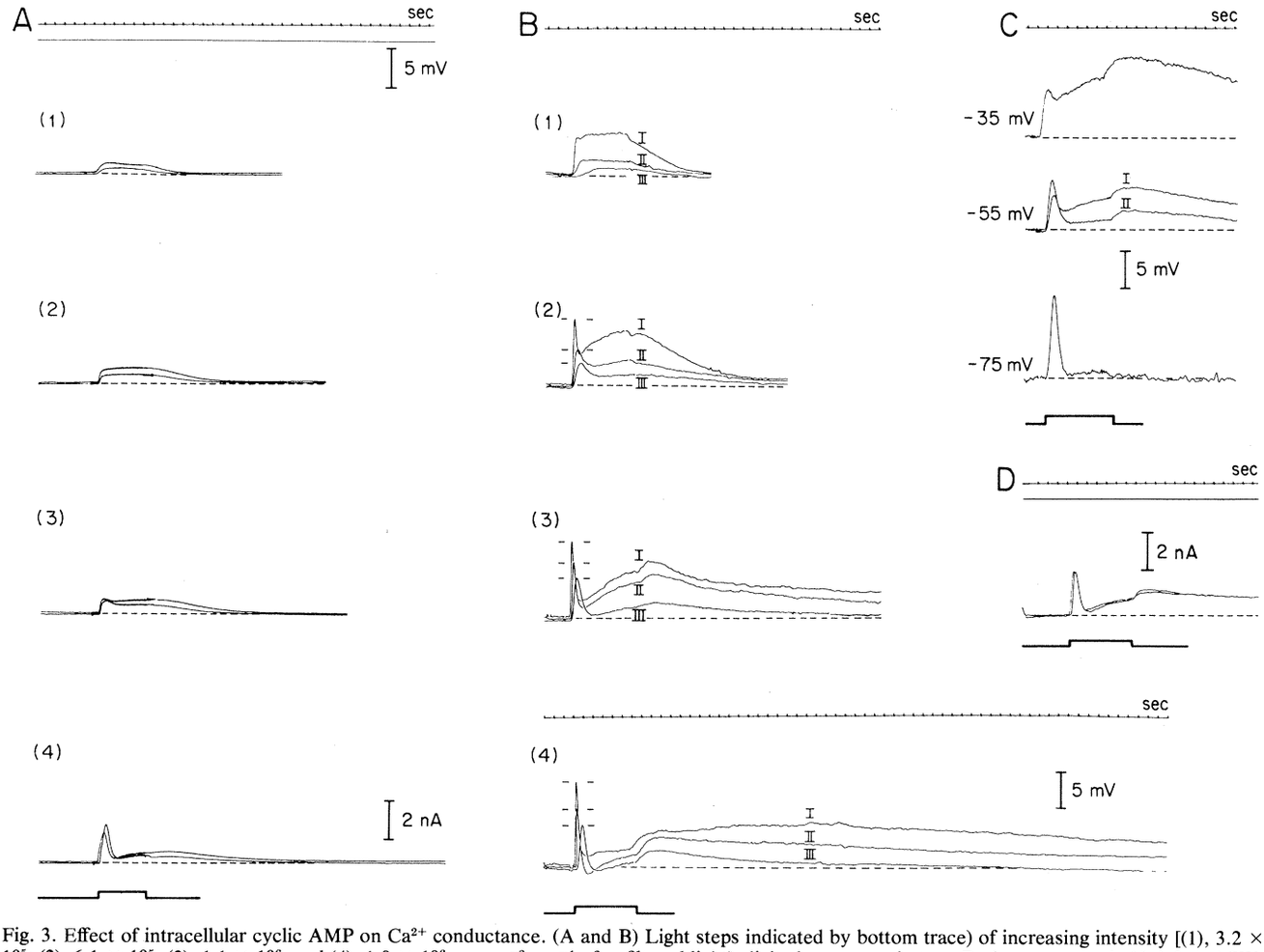

Fig. 3. Effect of intracellular cyclic AMP on Ca^{2+} conductance. (A and B) Light steps indicated by bottom trace) of increasing intensity [(1), 3.2 × 10^5; (2), 6.1 × 10^5; (3), 1.1 × 10^6; and (4), 1.8 × 10^6 erg cm^{-2} sec^{-1} of unfiltered light] elicited responses in type B photoreceptor in Na^+-free ASW. (A) Under voltage clamp at −20 mV, net inward currents elicited by light [upper recordings, (1) through (4)] were reduced (lower recordings) after intracellular injection of cyclic AMP (−0.5 nA for 1 minute). Top trace shows no voltage changes recorded under voltage-clamp conditions. (B) Voltage responses for different type B cell were also reduced after intracellular injection of cyclic AMP: I, before injection; II, after first injection, −0.2 nA for 1 minute; III, after second injection, −0.2 nA for 1 minute. (C) Voltage responses (in Na^+-free ASW) for third type B cell current clamped at holding potentials indicated on left. Light step intensity: 1.8 × 10^6 erg cm^{-2} sec^{-1} of unfiltered light; I, before, and II, after injection of cyclic AMP (1 minute, −0.2 nA). Currents of −0.2 nA displaced membrane potential to −75 and −35 mV, respectively. The late depolarizing response is enhanced at −35 mV and is absent at −75 mV. (D) Voltage responses for fourth type B cell, before and after injection of 5′-AMP (1 minute, 0.5 nA). Injection has little or no effect; light intensity as in (C). Note the absence of a hyperpolarizing voltage wave and an outward current during the least intense light step in (B) and (A).

cellular Ca^{2+}, and the Na^+ current suppressed by Ca^{2+} (*17*) (Fig. 1B) only at holding potentials > RP. Although the late outward current probably consists mainly of a Ca^{2+}-dependent K^+ current, at holding potentials ≤ RP an apparent late outward current could also result from inactivation of a resting Na^+ or Ca^{2+} current present in the dark.

Out of voltage clamp, the photoreceptor depolarizes by ~ +35 mV in response to the same intensity of light step used for the voltage-clamp recordings (Fig. 1, A and B) and then the photoreceptor shows LLD after the light step. This LLD and its associated increased membrane resistance (*8*) (Fig. 4A) cannot be explained by a net outward current at −20 mV under voltage clamp. That is, the LLD voltage response must arise from a voltage-dependent process that cannot occur when the voltage is held constant as it is under voltage clamp. The process which was most obviously voltage-dependent was the light-induced Ca^{2+} current. When the potential of the photoreceptor becomes increasingly negative (out of voltage clamp) after a light step, the light-induced Ca^{2+} current becomes progressively smaller. Similarly, as the photoreceptor repolarizes after a light step, the K^+ current which depends on the light-induced Ca^{2+} current decreases at a faster rate. These events provide a reasonable basis for the LLD: a slowly decreasing light-induced Ca^{2+} conductance and a potential-dependent light-induced K^+ conductance that decreases rapidly after a light step. These conductance changes would cause depolarization (the LLD) as well as the associated increased membrane resistance. The decreased K^+ conductance during the LLD may be due to an increase in intracellular Ca^{2+} as was suggested for another outward current (*19*). Thus, while a light-induced rise of intracellular Ca^{2+} may cause or facilitate a light-induced K^+ conductance, it may, after a light step, reduce K^+ conductance normally present in darkness. This could explain why in 1 m*M* Ni^{2+} the LLD occurred with reduced magnitude and for some of its duration without an associated increase in membrane resistance (Fig. 4A).

The potential dependence of the Ca^{2+} and the Ca^{2+}-dependent K^+ conductances is also consistent with the potential dependence of the LLD (*5*). That the LLD increases at more positive membrane potentials explains the effect of stimulus pairing. After light was paired with rotation, depolarization of the type B photoreceptor (LLD) increased (*8*). Stimulus pairing (Fig. 5) was always followed by greater depolarization and increased firing of the type B cell than with either stimulus alone or than the summed depolarization following the individual stimuli. Type B impulse activity and depolarization was al-

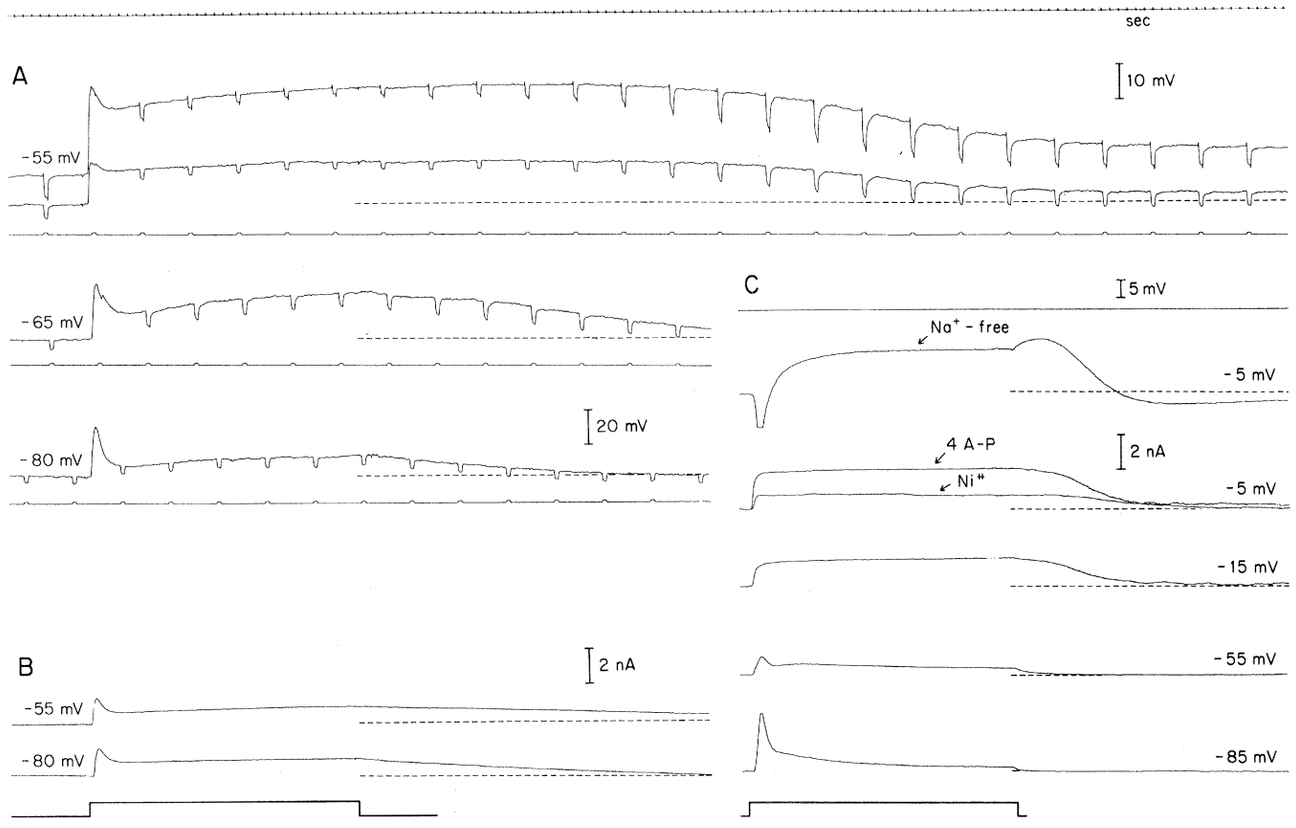

Fig. 4. Effects of blocking agents on voltage and voltage-clamp recordings during and after light steps. (A) Voltage recordings from type B cell in ASW containing 1 m*M* $NiCl_2$. Two microelectrodes recorded voltage simultaneously (upper two recordings). Current pulses injected through one microelectrode via a bridge circuit caused smaller voltage change during light (compared to before light) and transiently a larger voltage change (compared to voltage change before light); this indicates decreased membrane resistance after light (compared to membrane resistance before light). The LLD after light persisted in $NiCl_2$ when membrane resistance was not elevated. This was not so without $NiCl_2$. The LLD was reduced at more negative potentials (produced by injecting steady negative current through one microelectrode); light intensity (indicated by bottom trace), 1.1×10^6 erg cm^{-2} sec^{-1} (unfiltered). (B) Voltage-clamp recordings from same cell as in (A) under same conditions at comparable holding potentials; up = inward current. Note the long-lasting inward current after light step. Voltage traces at top were recorded simultaneously with current recordings. (C) Voltage-clamp recording during and after light steps in presence of blocking agents. Voltage traces at top were recorded simultaneously with current recordings. Upper recordings [in Na^+-free ASW, 1 m*M* 4-aminopyridine (*4 A-P*), and 1 m*M* $NiCl_2$] were all at −5 mV absolute holding potential. Current records at lower holding potentials were for same cell in 4-aminopyridine. Note absence of measurable early or late outward currents during and after light (intensity, 1.8×10^6 erg cm^{-2} sec^{-1}, unfiltered), and presence of slowly decreasing sustained inward current (Ca^{2+}). Dashed line indicates steady-state current level in darkness.

so substantially increased in those animals that had received the associative training paradigm, but not in those that had received the randomized control paradigms (*6*). These and other experiments (*5, 6*) suggest a possible causal relationship of increased type B activity and decreased velocity of movement toward a light source for intact animals.

What is the cellular mechanism by which type B impulse frequency increases in darkness with the learning paradigm? These data are consistent with primary modification (during training) of the type B membrane properties. This primary modification is observable as a long-lasting nonsynaptic depolarization of this photoreceptor (*6*). Let me suggest how this occurs.

Because of the synaptic interactions within and between the visual and statocyst pathways (Fig. 5A), rotation paired with light is followed by disinhibition of the type B cell (*8*) and an increased number of excitatory postsynaptic potentials (EPSP's) in this cell (*20*). Because membrane resistance (and thus the membrane time constant) is increased following a light step, the synaptic depolarization (due to disinhibition and the EPSP's) is enhanced (*8, 21*). The synaptic depolarization following stimulus pairing, however, also facilitates the light-induced depolarization which the present study indicates arises from voltage-dependent Ca^{2+} and K^+ conductances.

Thus, a kind of regenerative or positive feedback phenomenon is implicated for the mechanism of our associative learning model. Light-induced depolarization enhances stimulus pairing-induced synaptic depolarization which in turn enhances the light-induced depolarization, and so forth. With each successive trial, residual depolarization could potentiate and add to depolarization following the next stimulus pair. For behavioral and neural changes lasting for days, this depolarization may be both considerable and fairly permanent. It will be of interest to further investigate the relationship of cyclic AMP to these findings, particularly with respect to long-term modification of animal behavior. Intracellular Ca^{2+} and cyclic nucleotide levels are now thought to have regulatory effects on each other in a number of tissues (*22*). Intracellular Ca^{2+} could control enzymes which catalyze the synthesis (*23*) or the degradation of cyclic nucleotides. Cyclic nucleotides, in turn, could control Ca^{2+} and H^+ pumping mechanisms (*24, 25*).

Thus far, at least two distinct neurophysiologic functions have been suggested for Ca^{2+}-cyclic nucleotide interaction. One concerns phototransduction or adaptation properties of photoreceptors (*24*); the other involves mediation of synaptic transmission (*26*). As an extension of the latter function, heterosynaptic facilitation might depend on presynaptic enhancement of Ca^{2+} influx by cyclic AMP (*27*).

A possible means for, or expression of, Ca^{2+}-cyclic nucleotide interaction might be provided by intracellular phosphorylation of proteins. There is evidence, for instance, of cyclic nucleotide-dependent phosphorylation of proteins in retinal rods (*28*), Ca^{2+}-dependent protein phosphorylation in neural membranes (*29*), depolarization-induced protein phosphorylation mediated by Ca^{2+} influx in synaptosomes (*30*), and light-dependent phosphorylation of rhodopsin (*31*). Phosphorylation of proteins would not be an unreasonable biochemical mechanism for the long-lasting behavioral changes of *Hermissenda* produced by the associative learning procedures. It is possible, for instance, that in the type B photoreceptor intracellular cyclic AMP regulates protein phosphorylation which in turn is responsible for the light-induced Ca^{2+} conductance and Ca^{2+}-dependent K^+ conductances. Associative training may affect intracellular cyclic AMP levels and membrane protein phosphorylation. This in turn might cause accumulation of intracellular Ca^{2+} and reduced K^+ conductance ultimately

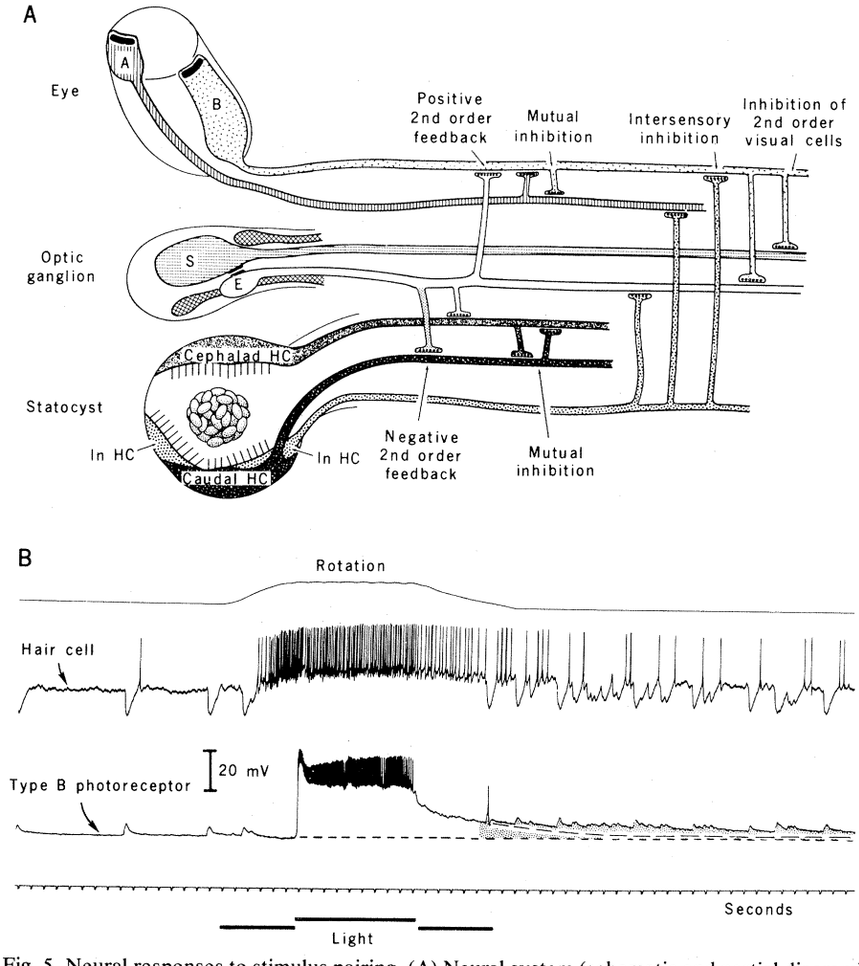

Fig. 5. Neural responses to stimulus pairing. (A) Neural system (schematic and partial diagram) responsive to light and rotation. Each eye has two type A and three type B photoreceptors; each optic ganglion has 13 second-order visual neurons; each statocyst has 12 hair cells. The neural interactions (intersection of vertical and horizontal processes) identified to be reproducible from preparation to preparation are based on intracellular recordings from hundreds of pre-and postsynaptic neuron pairs. Abbreviations; *In HC*, hair cell ~45° lateral to caudal north-south equatorial pole of statocyst; *S*, silent optic ganglion cell, electrically coupled to E cell; *E*, optic ganglion cell, presynaptic source of EPSP's in type B photoreceptors. The E second-order visual neuron causes EPSP's in type B photoreceptors and cephalad hair cells and simultaneous inhibitory postsynaptic potentials (IPSP's) in caudal hair cells. (B) Intracellular recordings (simultaneous) from caudal hair cell and type B photoreceptor shows increase of EPSP's (type B cell, lower record) and simultaneous IPSP's (caudal hair cell, upper record) after light paired with rotation. The LLD after stimulus pairing is greater that that after light alone (line of long dashes). The line of short dashes indicates level of resting membrane potential. The lowest trace indicates light duration; top trace, angular velocity of turntable (effecting 1.2*g*).

causing depolarization of the type B cell. Analysis of protein phosphorylation in the type B cell, particularly in relation to the training procedures described, may eventually suggest specific biochemical steps within the associative learning procedure for *Hermissenda* and possibly for more evolved species.

DANIEL L. ALKON

Section on Neural Systems, Laboratory of Biophysics, Intramural Research Program, National Institute of Neurological and Communicative Disorders and Stroke, Marine Biological Laboratory, Woods Hole, Massachusetts 02543

References and Notes

1. N. E. Miller, *Proc. Am. Philos. Soc.* **111**, 315 (1967); in *The Neurosciences: A Study Program*, G. C. Quarton, T. Melnechuk, F. O. Schmitt, Eds. (Rockefeller Univ. Press, New York, 1967), vol. 2, p. 643.
2. D. L. Alkon, *J. Gen. Physiol.* **64**, 70 (1974); T. J. Crow and D. L. Alkon, *Science* **201**, 1239 (1978).
3. J. Harrigan, T. Crow, D. L. Alkon, unpublished observations; D. L. Alkon, *Sci. Am.*, in press.
4. M. J. Dennis, *J. Neurophysiol.* **30**, 1439 (1967); D. L. Alkon and M. G. F. Fuortes, *J. Gen. Physiol.* **60**, 631 (1972); D. L. Alkon, *ibid.* **61**, 444 (1973); *ibid.* **62**, 185 (1973); *ibid.* **66**, 507 (1975); *ibid.* **67**, 197 (1976); ———, T. Akaike, J. Harrigan, *ibid.* **71**, 177 (1978); L. J. Stensaas, S. S. Stensaas, O. Trujillo Cenoz, *J. Ultrastruct. Res.* **27**, 510 (1969).
5. D. L. Alkon, *J. Gen. Physiol.* **65**, 46 (1975); *ibid.* **68**, 341 (1976).
6. T. Crow and D. L. Alkon, *Soc. Neurosci. Abstr.* **4**, 191 (1978).
7. Photoreceptors had axons cut either at their exit point from the eye (leaving essentially the isolated somata) or ~ 30 to 40 μm from the exit point. These lesions (*8*) eliminated all synaptic interactions and impulses of the photoreceptors. Input resistance usually increased slightly for such cells. Occasionally, residual impulse activity was observed with the cut 40 μm from the exit point (Fig. 1C). Current and voltage records were otherwise identical for these two types of preparations.
8. D. L. Alkon and Y. Grossman, *J. Neurophysiol.* **41**, 1328 (1978).
9. W. J. Adelman, Jr., and Y. Palti, *J. Gen. Physiol.* **53**, 685 (1969).
10. Absolute values of holding potential are given assuming an RP of −55 mV; RP was not measured precisely each time but there was a variation of ± 10 mV when it was determined.
11. The maximum frequency response of this instrument (100 Hz for 1 cm, 40 Hz for 4 cm) was adequate for the relatively slow current and voltage responses of interest.
12. A photosensitive peak at 509 nm [D. L. Alkon, in *Neural Principles of Vision*, F. Zettler and R. Weiller, Eds. (Springer-Verlag, Berlin, 1976), p. 410] has been determined for type B cells. Because the light source used here emitted only a small percentage of its light at or near this wavelength, high source intensities were necessary (10^5 to 10^6 erg cm^{-2} sec^{-1}). These intensities (4-second steps) caused no measurable (± 0.1°C) changes of bath temperature; 30-second light steps (10^6 erg cm^{-2} sec^{-1}) caused a photoreceptor LLD response (Fig. 1A) comparable to that elicited (*8*) by a quartz-iodide source (10^4 erg cm^{-2} sec^{-1}) with no measured temperature change. Light filtered by a 500 ± 10 nm narrow-band interference filter (Oriel, Stamford, Conn.) produced, at sufficient intensities (10^1 to 10^3 erg cm^{-2} sec^{-1}), essentially identical photoreceptor voltage and current responses.
13. Artificial seawater (ASW) contained Na^+, 482.5 m*M*; K^+, 10 m*M*; Mg^{2+}, 55 m*M*; Ca^{2+}, 10 m*M*; Cl^-, 620 m*M*; and tris buffer, 10 m*M* (*p*H 7.2).
14. Although light-induced Ca^{2+} inward currents were previously not clearly observable in other photoreceptors with voltage clamp experiments, their presence has been inferred or monitored with other techniques by previous workers [H. M. Brown, S. Hagiwara, H. Koike, R. M. Meech, *J. Physiol. (London)* **208**, 385 (1970); J. E. Brown and J. R. Blinks, *J. Gen. Physiol.* **64**, 643 (1974)]. That the sustained light-induced inward current is carried by Ca^{2+} across the type B photoreceptor membrane was confirmed by the observation that it was present in 120 m*M* K^+, Na^+-free ASW at the K^+ reversed potential (Figs. 1B, bottom, and 2C), as well as in Na^+-free ASW at the approximate reversal potentials for Na^+ and Cl^- currents (Fig. 1, D and E, and Fig. 2, A and B).
15. S. Hagiwara, in *Membranes*, G. Eiseman, Ed. (Dekker, New York, 1975), vol 3, p. 359.
16. Y. Grossman and D. L. Alkon, in *Abstracts, 6th International Biophysics Congress, 1978*, in press; J. A. Schmidt, Y. Grossman, D. L. Alkon, *Biophys. J.* **21**, 136a (1978); P. B. Detwiler, *J. Physiol. (London)* **256**, 691 (1976).
17. Y. Grossman, J. A. Schmidt, D. L. Alkon, in preparation. Grossman *et al.* (*16*) have presented substantial evidence for a K^+ current which results from increased intracellular Ca^{2+} during a hyperpolarizing wave in the type B light response and for a Ca^{2+}-suppressed Na^+ current during the depolarizing light response. They determined a reversal potential for the hyperpolarizing wave, and used K^+ and Ca^{2+} blocking agents and injection of Ca^{2+} and EDTA.
18. R. W. Meech, *Comp. Biochem. Physiol.* **42A**, 493 (1972); *J. Physiol. (London)* **237**, 259 (1974); ——— and N. B. Standen, *ibid.* **249**, 211 (1975); K. Krnjevic and A. Lisievicz, *ibid.* **225**, 363 (1972); K. Krnjevic, E. Puil, R. Werman, *Can. J. Physiol. Pharmacol.* **53**, 1214 (1975); A. M. Brown, M. S. Brodwick, D. C. Eaton, *J. Neurobiol.* **8**, 1 (1975); M. V. Thomas and A. L. F. Gorman, *Science* **196**, 531 (1977); C. B. Heyer and H. D. Lux, *J. Physiol (London)* **262**, 340 (1977); in *Abnormal Neural Discharges*, N. Chalazonitis and M. Boisson, Eds. (Raven, New York, 1978), p. 311.
19. R. Eckert and H. D. Lux, *Science* **197**, 422 (1977).
20. M. Tabata and D. L. Alkon, *Invest. Ophthalmol. Vis. Sci. Suppl.* (1979), p. 77.
21. W. Rall, J. Rinzel, R. Miller, D. Alkon, in preparation.
22. H. Rasmussen, *Science* **170**, 404 (1970); ———, P. Jensen, W. Lake, N. Friedman, D. B. P. Goodman, *Adv. Cyclic Nucleotide Res.* **5**, 375 (1975); M. J. Berridge, *ibid.* **6**, 1 (1976).
23. H. Rasmussen and D. B. P. Goodman, *Ann. N.Y. Acad. Sci.* **253**, 789 (1975).
24. W. J. Malaisse, *Diabetologica* **9**, 167 (1973); A. B. Barle, *J. Membr. Biol.* **16**, 221 (1974); S. A. Lipton, H. Rasmussen, J. D. Dowling, *J. Gen. Physiol.* **70**, 771 (1977).
25. W. Boron, J. Russell, M. Brodwick, D. Keifer, A. Roos, *Nature (London)* **276**, 511 (1978).
26. D. A. McAfee and P. Greengard, *Science* **178**, 310 (1972); H. Kobayashi, T. Hashiguchi, N. S. Ushiyama, *Nature (London)* **271**, 268 (1978); J. P. Gallagher and P. Shinnick-Gallagher, *Science* **198**, 851 (1977).
27. T. Shimahara and L. Tauc, in *Trosieme Collogue de Royaumont* (Centre National de la Recherche Scientifique, Paris, 1975), p. 18; *Brain Res.* **118**, 142 (1976); *ibid.* **127**, 168 (1977); *J. Physiol. (Paris)* **74**, 515 (1978); M. Klein and E. Kandel, *Proc. Natl. Acad. Sci. U.S.A.*, **75**, 3512 (1978).
28. D. B. Farber, M. B. Brown, R. N. Lolley, *Biochemistry* **18**, 378 (1979).
29. H. Schulman and P. Greengard, *Proc. Natl. Acad. Sci. U.S.A.* **75**, 5432 (1978).
30. B. K. Krueger and P. Greengard, *J. Biol. Chem.* **252**, 2764 (1977).
31. H. Shichi and R. L. Somers, *ibid.* **253**, 7040 (1978).
32. I thank J. Shoukimas, R. French, W. Rall, J. Rinzel, R. Miller, and W. J. Adelman, Jr., for their helpful discussions. I am particularly grateful to J. Neary for his suggestions concerning the cyclic AMP experiments.

29 January 1979; revised 20 April 1979

5-Bromodeoxyuridine Inhibits Sequence Changes Within Inverted Repeat DNA During Embryogenesis

Abstract. *Previous studies on the genome of* Strongylocentrotus purpuratus *sea urchin have shown that changes in the nucleotide sequence of inverted repeat sequences occur during embryogenesis. The present study indicates that these sequence changes fail to occur when the embryos are raised in the presence of 5-bromodeoxyuridine. This drug is an analog of thymidine, is incorporated into the DNA during embryogenesis, and inhibits cell differentiation in these embryos.*

Previous experiments on *Strongylocentrotus purpuratus* sea urchin embryos suggest that there are sequence changes during embryogenesis within inverted repeat DNA sequences in the genome (*1*); we now show that these sequence changes do not occur when sea urchin embryos are cultured in the presence of 5-bromodeoxyuridine (BrdU).

Incorporation of the thymidine analog BrdU into DNA arrests differentiation in many biological cells (*2*), including *S. purpuratus* embryos (*3, 4*). With 50 μg of BrdU per milliliter of seawater media present from the time of fertilization of these embryos, development is altered at gastrulation (*3*), numerous anatomical changes occur prior to the completion of blastulation (*3, 4*), 30*S* to 60*S* duplex DNA pieces accumulate during the cleavage period of development (*5–7*), and BrdU replaces as much as 41 percent of the thymidine in the embryo DNA by the time that development has reached morula stage (*7*).

We have tested inverted repeat DNA sequences for sequence changes during embryogenesis by comparing the bulk adjacent inverted repeats taken from *S. purpuratus* sea urchin embryos at different stages of development (*1*). When isolated, sheared, sea urchin DNA is denatured and renatured at $< 10^{-4}$ C_0t (moles of nucleotide per liter times time in seconds) and the duplex DNA is collected on hydroxyapatite, the final DNA preparation recovered after three rounds of this renaturation is largely hairpin-like in structure (*1*); the hairpins are formed by foldback with subsequent intrastrand hydrogen-bonding of those homologous sequences that are inverted relative to each other and are adjacent or nearly so on the same strand of DNA (*1, 8, 9*). Folding of isolated strands of inverted repeat DNA in vitro causes base-pair mismatches to be formed at points on the stems of the hairpins wherever there are departures in the homology of the left and right arms of the individual adjacent

0036-8075/79/0824-0816$00.50/0